Title: The NPxY motifs in the β integrin regulates serotonin response and mechanosensation in *C. elegans*.

Josh Haram Bumm*, Daniel Dogeon Lee*, Zhongqiang Qiu, Angela Choi, Meghana Kolluri, Michael J. Olsen, Lianzijun Wang, and Myeongwoo Lee#

Department of Biology, Baylor University, Waco, Texas 76798, USA.

Keywords: phosphomimetic, disruptive, tyrosine phosphorylation, serotonin transporter, fluoxetine,

Running title: Role of integrin NPxY motifs in egg laying and mechanosensation.

* These authors contributed equally to the work.
#To whom all correspondence should be addressed,
Myeongwoo Lee, Ph.D.
Department of Biology
Baylor University, Waco, TX 76798
Email) Myeongwoo_Lee@baylor.edu

## ABSTRACT

Integrin is an αβ heterodimeric receptor; its binding to the matrix recruits focal adhesions to two NPxY (Asn-Pro-x-Tyr) motifs, the putative tyrosine phosphorylation sites in the cytoplasmic domain. Here, we report a novel role for *pat-3* β integrin NPxY motifs in *C. elegans*. The double non-phosphorylatable *pat-3(YYFF)* mutant exhibited an egg-laying defect, accumulating more unlaid eggs in the uterus while still responding to serotonin or fluoxetine. The phosphomimetic distal *pat-3(Y804E)* mutant also displayed a reduced response to serotonin and fluoxetine, suggesting phosphorylation of the distal NPxY motif is associated with vulval contraction. Additionally, the non-phosphorylatable *pat-3(Y792F)*, *pat-3(YYFF)*, disruptive *pat-3(Y792A)*, and phosphomimetic *pat-3(Y804E)* mutants exhibited mechanosensation defects, demonstrating that NPxY phosphorylation regulates sensory responses.
Our results underscore the functional importance of *pat-3* NPxY motifs in muscle and sensory neurons, potentially linking integrin NPxY motifs to muscle anomalies and mechanosensory functions.

# INTRODUCTION

Integrin is an αβ heterodimeric cell surface receptor to the extracellular matrix (ECM), controlling cell behaviors through bidirectional signaling. Inside-out signaling activates the integrin extracellular domain to facilitate ECM binding, while outside-in recruits signaling molecules and links cytoskeletons to the cell-ECM contacts, known as focal adhesions (FAs) [1]. In this context, the cytoplasmic domain (CTD) of β integrin interacts with linker proteins such as talins and kindlins to transduce mechanical information from the ECM to the cell [2]. Two conserved NPxY motifs, potential tyrosine phosphorylation sites, are present in the CTD of all metazoan β integrins [3]. The membrane proxy NPxY binds to the FERM domain of talin, while the membrane distal motif interacts with kindlin [4]. Sakai *et al.* reported overexpression of *src* kinase in a mouse fibroblast phosphorylated the NPxY motifs of β1A integrin [5]. In mice, knock-in β1 integrin YYFF (Tyrosine-to-Phenylalanine) failed to exhibit discernible phenotypes [6], although these mutants showed resistance to tumorigenesis [7] and defects in blood clotting [8]. Conversely, disruptive β1 YYAA, Y783A, or Y795A (Tyrosine-to-Alanine) mutations caused severe phenotypes, including embryonic lethality [6]. These findings suggest that the Y-to-A transition generally brings severe phenotypes to the animal, while the Y-to-F produces no overt developmental phenotypes.

In the nematode *C. elegans*, PAT-3/β integrin is ubiquitously localized in tissues, including body wall muscles, gonads, neurons, vulva, and the excretory canal [9]. PAT-3 integrin also contains two NPxY motifs [10]. Previous analyses by Itoh *et al.* suggested that SRC family tyrosine kinases (SFK) could phosphorylate the *pat-3* CTD. For instance, the *C. elegans src-1* mutant exhibited gonad phenotypes similar to those caused by the integrin HA-βtail dominant negative allele [10,11]. Our recent study demonstrated that mutations in the membrane distal Y to A, E (glutamic acid), or F mutations resulted in gonad migration and mild motility impairments [12]. These findings suggest that phosphorylation of the membrane distal NPxY is dispensable for development and motility. However, given the widespread distribution of integrins in

muscle, neurons, and gonads, we hypothesized that the NPxY motifs in PAT-3 CTD are crucial in tissue-specific functions.

In *C. elegans* hermaphrodites, vulva development begins at the L1 larval stage and culminates at the late larval stages. At the early adult stages, oocytes undergo fertilization, and fertilized eggs accumulate in the uterus. Within eight hours of post-fertilization, the fertilized eggs are expelled from the uterus through vulva contractions, a process known as 'egg laying' [13]. Egg laying in *C. elegans* is regulated by a pair of serotonergic hermaphrodite-specific motor neurons (HSNs) connected to vulva muscles. During egg laying, the HSN releases a neurotransmitter, serotonin, onto the vulva muscle, inducing their contractions. When the serotonin production or its receptor is defective, the vulva muscles fail to contract, resulting in the accumulation of unlaid eggs in the uterus and causing the Egl (egg-laying defective) phenotype. Treating worms with exogenous serotonin or serotonin reuptake inhibitors stimulates vulva muscle contraction and increases egg-laying [13]. Several *C. elegans* mutants displayed the Egl phenotype. Mutations in the genes associated with muscle attachment [14], such as βPAT-3 RNAi [13,15], perlecan/UNC-52 [16,17], and syndecan/SDN-1 [18], have been reported to cause defective egg laying, suggesting a link between the Egl phenotype and impaired cell-ECM interactions.

In *C. elegans*, gentle touch on the body induces either backward or forward movement. The touch stimulus is detected by six touch receptor neurons (TRNs): ALMR, ALML, AVM, PLMR, PLML, and PVM [19]. These TRNs express the MEC-4 DEG/ENaC channel complex on their cell surfaces, transmitting touch stimuli to the neurons. Extensive studies have identified several *mec* (mechanosensation abnormal) genes essential for processing touch-induced behaviors [20]. Integrins and focal adhesion proteins transmit mechanical forces and trigger cellular signaling responses [21]. Focal adhesion proteins are expressed in mechanosensory cells, including TRNs [22]. Studies on focal adhesion genes—such as *unc-97/PINCH* [23] mutant and removal of *pat-2*/α integrin [24], *pat-3*/β integrin [10], *pat-6*/actopaxin [25], and *unc-112*/kindlin [26]—in ALM and PLM touch neurons

of genetic mosaic animals demonstrated the involvement of these genes in mechanosensation n [22].

In this study, our results revealed that the phosphomimetic *pat-3 (kq8042, Y804E)* mutation exhibited defective egg-laying in response to serotonin or fluoxetine treatment. Conversely, the *pat-3(kq7923, Y792F)* mutant was hypersensitive to serotonin. In contrast, the non-phosphorylatable *pat-3(kq24, YYFF)* mutant displayed a wild-type response to serotonin and fluoxetine treatment, accompanied by increased egg retention. Further investigation into the role of *pat-3* NPxY motifs revealed that *pat-3(kq7921, Y792A)*, *pat-3(kq7923, Y792F)*, *pat-3(kq24, YYFF)*, and *pat-3(kq8042, Y804E)* mutants exhibited touch insensitivity in the anterior or posterior regions of the body. These findings suggest that phosphorylation of the NPxY motif is critical for modulating both egg-laying and mechanosensation.

## RESULTS

*Mutations in the βpat-3 NPxY motifs.*

To characterize the phosphorylation of the NPxY motif in the β*pat-3* CTD, we introduced mutations into the membrane-distal NPxY in the βPAT-3 CTD (Figure 1A). Previous analyses revealed that CRISPR edits in the membrane-distal NPxY of βPAT-3 led to motility and gonad migration defects [12]. We generated *pat-3(kq24, YYFF)*, a non-phosphorylatable mutation, to investigate the impact of NPxY phosphorylation removal. Most of the *pat-3* NPxY mutants exhibited regular muscle filament organization. Some mutants were crossed with AH3437 *GFP::tln-1* [27] to visualize the structure of dense bodies and M lines (Figure 2, panels A to F). Except for *pat-3(kq7921, Y792A)* in Figure 2E, all viable mutants displayed dense bodies and M lines along the body wall, suggesting that the mutations were dispensable for organizing cell attachment structures.

*Membrane distal NPxY appears to regulate egg-laying behavior.*

When the hermaphrodite is submerged in an aqueous solution, it pauses egg laying because worms recognize the environment as a lack of food [28]. Adding exogenous serotonin into the solution would induce egg laying [13]. Before egg-laying assays of the NPxY mutants, the fecundity of viable NPxY mutants, along with N2 and other control mutants, was assessed to determine the optimal period to measure the egg laying (Figure S1). All worm strains showed the peak number of eggs laid on Day 2. Therefore, the egg-laying behavior was measured with Day 2 hermaphrodites.

To monitor the egg-laying of the *pat-3* NPxY mutants, we incubated adult hermaphrodites in 3.0 mg/ml serotonin dissolved in M9 buffer. After one hour incubation, *pat-3(kq8042, Y804E)*, the phosphomimetic mutant, laid significantly less eggs in the serotonin solution than N2 ($p < 0.0001$, n = 50). The *pat-3(kq8043, Y804F),* the distal non-phosphorylatable, and *pat-3(kq9-41, Y804A)*, the distal disruption,

mutants showed comparable egg laying to N2 ($p < 0.8$) (Figure 3, Supplementary Table 3).

We also treated the mutants with 0.5 mg/ml of fluoxetine, a serotonin reuptake inhibitor, to stimulate egg laying [29]. Fluoxetine binds to MOD-5/CeSERT, the serotonin reuptake transporter (SERT) on neurons (presumably on the HSN), inhibits the function of the SERT, and increases the endogenous serotonin [30]. The egg laying of *pat-3(Y804E)* in fluoxetine was defective ($p < 0.0001$), suggesting that the defective egg laying of the mutant in serotonin and fluoxetine was due to vulva contraction defects (Figure 3, Supplementary Table 3). As a comparison, the membrane-proximal *pat-3 (kq7923, Y792F)* was also generated to compare the role of two NPxY motifs. The *pat-3(Y792F)* worms showed a much higher egg-laying response to serotonin than N2 *($p < 0.0001$)*. In contrast, the same mutant showed less sensitivity to fluoxetine than N2 *($p < 0.0016$)*.

*Some NPxY mutants retained fewer unlaid eggs in the uterus than N2.*

Due to the delayed release, defective egg laying (Egl) mutants harbor more unlaid eggs in the uterus than N2 [31]. Fertilized eggs are released from the uterus before reaching the 48-cell stage embryo [32]. The Egl animals also retain unlaid eggs from the late stages of embryogenesis, such as the two-fold or comma stage in the uterus. We measured the number of unlaid eggs in the uterus (Figure 4, Supplementary Tables 4 and 5). The number of unlaid eggs in most NPxY mutants was comparable to that in N2. However, *pat-3(Y792F)* displayed fewer unlaid eggs in the uterus than N2 ($p < 0.0019$, n = 50) or the other mutants. This analysis showed that *pat-3(Y792F)* retained fewer eggs in the uterus while laying more eggs in serotonin stimulations, suggesting that the egg laying is accelerated.

To investigate the egg retention anomalies among the mutants, we also examined the embryonic stages of unlaid eggs. In N2 animals, all eggs were laid out of the body before the gastrulation [32]. Therefore, we looked for embryos at the two-fold, comma, or older stage among the unlaid eggs. Fewer than several eggs in N2 animals (1.0 eggs

per animal) were scored for post-comma stage embryos, defined as late-stage. In contrast, the number of late-stage eggs increased in *pat-3(Y792F), pat-3(Y804E),* and *pat-3(Y804F)* mutants ($p < 0.0001$) (Figure 4).

*Double non-phosphorylatable NPxY showed a distinct egg-laying phenotype.*

The defective egg-laying in the distal NPxY mutants prompted us to examine the effect of dephosphorylation. In mammalian studies, the homologous knock-in of YY to FF in mice β1 and β3 integrins showed no overt behavioral defects [6]. The *pat-3(kq24, YYFF)* laid a comparable number of eggs in serotonin or fluoxetine during the sixty minutes of incubation, suggesting that the egg-laying appeared similar to N2 (for serotonin, $p < 0.99$, and fluoxetine $p < 0.88$) (Figure 3, Supplementary Table 3). However, the egg retention of *pat-3(YYFF)* showed a higher number of unlaid eggs in the uterus than in N2 ($p < 0.0001$). The *pat-3(YYFF)* carried about thirty percent more unlaid eggs than N2 animals (Figure 4). This result suggested that *pat-3(YYFF)* animals also delayed egg-laying while capable of vulva contraction in response to serotonin or fluoxetine.

The mechanosensation of β*pat-3* integrin NPxY mutants.

*C. elegans* egg laying is a complex behavior that requires the coordination of multiple muscles and neurons, including vulva and uterine muscles and HSN and VC motor neurons [33]. While the current study primarily focuses on contractile tissues, our results implied the potential involvement of integrin in neurons linked to egg laying.

In *pat-3(Y804E)*, serotonin treatment failed to improve egg laying to N2 levels, although egg retention fell within the normal range of 10 to 15 [33] (Figures 3 and 4). The *pat-3(Y792F)* and *pat-3(Y804A)* mutants were more or equally sensitive to serotonin compared to N2 ($p < 0.0001$ and $p < 0.87$, respectively), but both were less sensitive to fluoxetine than N2 ($p < 0.0001$ and $p < 0.01$). In contrast, *pat-3(YYFF)* displayed egg-laying levels comparable to N2 in both treatments while exhibiting a higher accumulation of unlaid eggs than N2 ($p < 0.0001$). This suggests that their altered behavior may result from reduced neurotransmitter production or impaired ability to

initiate egg-laying due to decreased sensitivity to mechanical stimuli from surrounding tissues (Figure 3).

Several studies demonstrated connections among mechanosensation, egg laying, and integrin. Chalfie *et al.* (1985) identified a pair of PLM touch neurons extending along the posterior lateral side and synapse with the HSN motor neurons [34]. Vibrational stimulation inhibited egg laying, and this response was dependent on the ALM and PLM touch neurons [35]. Ravie *et al.* (2018) proposed that mechanical pressure from egg accumulation in the uterus triggers egg laying through a potential homeostatic mechanism [36]. Chen and Chalfie (2014) demonstrated that *pat-3* mosaic animals showed defects in ALM [22]. These potential interactions among mechanosensation, egg laying, and integrin led us to hypothesize that the phosphorylation of integrin NPxY is crucial for touch response and that mutations in PAT-3 NPxY phosphorylation would result in a defective response to mechanical stimulations [37].

Therefore, we evaluated the NPxY mutants using gentle touch analyses [38] (Figure 5, Supplementary Table 5). Well-fed adult animals were prodded on the anterior or posterior half of the body [39,40]. The scoring involved assessing backing (anterior touch) or sprinting forward movement (posterior touch) after the touch stimulation [23]. Our results revealed that most NPxY mutants exhibited significantly decreased touch responses on the anterior or posterior side of the body (Figure 5). However, *pat-3(kq8041, Y804A)* and *pat-3(kq8043, Y804F)* appeared normal in response to gentle touch stimulations.

Two mutants, *pat-3(kq7923, Y792F)* and *pat-3(kq8042, Y804E),* were significantly touch insensitive (Figure 5, $p < 0.0001$ compared to N2 posterior), with the defect biased toward the posterior ends. To deepen the analysis of the involvement of membrane-proximal NPxY in mechanosensation, *pat-3(kq7921, Y792A)*, a disruptive mutation, was generated (see Materials and Methods). The $NPIA^{792}$ mutation caused a disruptive change, abolishing the structure of the intact membrane proximal motif. Although *pat-3(Y792A)* animals displayed severely uncoordinated movement with irregular and

patchy dense bodies (Figure 2E), they were viable and fertile. In addition, the touch response in *pat-3(Y792A)* was severely defective in both anterior and posterior bodies, suggesting that the proximal NPxY motif is also essential for motility and mechanosensation (Figure 5). The *pat-3(Y804A)*, disruptive distal NPxY mutant, however, failed to show touch insensitivities in both sides ($p < 0.2$).
The double non-phosphorylatable NPxY mutant, *pat-3(kq24, YYFF),* displayed significant anterior ($p < 0.0277$) and severe posterior touch insensitivity ($p < 0.0001$).
Next, we examined a mechanosensation mutant for egg-laying defects to explore the correlation between touch sensitivity and egg laying. The *mec-4(u253)* animal, a null allele of the MEC-4/ENaC mechanoreceptor [41], demonstrated severe touch defects in both ends (Figure 5), while it retained fewer unlaid eggs with more late-stage eggs than N2 ($p < 0.0222$) (Figure 4). While the egg-laying of *mec-4(u253)* in the serotonin did not differ from the wild type ($p < 0.995$, compared to N2), it failed to respond to fluoxetine ($p < 0.0001$) (Figure 3), suggesting *mec-4(u253)* has a decreased level of serotonin in the tissue.

# DISCUSSION

Our study elucidates the previously undescribed role of integrin NPxY motifs. Our data reveal varied egg-laying responses to serotonin and fluoxetine treatments among the *pat-3* alleles: *pat-3(Y804E), pat-3(YYFF)*, and *pat-3(Y792F)*. Functional analysis of the membrane-distal NPxY indicates that the *pat-3(Y804E)* phosphomimetic mutant significantly decreases egg laying on both drug treatments. In particular, the non-phosphorylatable *pat-3(YYFF)* allele exhibits normal egg-laying responses to serotonin or fluoxetine but retains more unlaid eggs in the uterus. Conversely, the membrane proxy *pat-3(Y792F)* mutant demonstrates reduced sensitivity to fluoxetine and retains fewer eggs than N2. Beyond egg-laying behaviors, these NPxY mutants display defective mechanosensation. This suggests that timely phosphorylation of the NPxY motif is critical for regulating vulva muscle contraction and touch receptor neuron function.

Our data demonstrate that *pat-3* NPxY is essential for responding to serotonin and fluoxetine. Our findings reveal that tyrosine phosphorylation disrupts vulva contraction, as observed in *pat-3(Y804E)*, suggesting that the membrane-distal Y804 residue may serve as a critical switch for serotonin and fluoxetine responses. This result indicates that the distal $NPVY^{804}$ potentially interacts with MOD-5/CeSERT and serotonin receptors. Phosphorylation of distal $NPVY^{804}$ may impair the function of MOD-5 or multiple serotonin receptors. Notably, Carneiro *et al.* (2008) reported that αIIbβ3 platelet integrin binds to the C-terminal domain of platelet SERT, where active β3 integrin enhances the serotonin transporter activity of the SERT [42].

The *pat-3(YYFF)* exhibits anomalies by accumulating more unlaid eggs while responding to serotonin and fluoxetine at the level of N2. This observation suggests that *pat-3(YYFF)* is defective in initiating egg-laying, possibly due to reduced mechanosensation of pressure from the oviparous uterus. The defect could arise from insufficient serotonin production to trigger vulva contraction [31] or the failure of utero-vulva feed-forward mechanism to stimulate egg-laying via serotonin secretion [43].

In contrast, the *pat-3(Y792F)* mutant displays hypersensitivity to serotonin but a reduced response to fluoxetine, implying that *pat-3(Y792F)* as well as *pat-3(Y804A)* decreases serotonin levels. In *C. elegans*, serotonin is secreted from NSM, ADF, and HSN neurons [44]. However, no evidence of serotonin production in muscles suggests that the NPxY phosphorylation regulates serotonin production in non-muscle cells. Interestingly, the egg retention phenotype of the phosphomimetic *pat-3(kq8042, Y804E)* resembles that of N2, indicating that constitutive phosphorylation of the distal motif specifically affects vulva muscle contraction. Fluorescence microscopy (Figure 2) reveals an organized talin distribution in the body wall muscle of the *pat-3(Y804E)* mutant, demonstrating that phosphorylation of the distal NPxY is dispensable for muscle organization. We conclude that an unknown factor downstream of *pat-3(Y804E)*, presumably *goa-1* [45], likely influences serotonin sensitivity and muscle contraction.

*Several NPxY mutants display defective mechanosensation.*

The *pat-3(kq24, YYFF)* and *pat-3(kq8042, Y804E)* alleles exhibit mechanosensation defects in both the anterior and posterior regions, whereas *pat-3(kq7923, Y792F)* shows the defect primarily in the posterior half. Our analysis suggests that NPxY phosphorylation modulates mechanosensation (see Figure 5). This finding aligns with anatomical studies by Chalfie *et al.* (1985), which revealed that mechanosensory PLM neurons form synapses with the HSN. Chen *et al.* (2014) demonstrated that *pat-3*$^{-/-}$ mosaic in ALM neurons exhibits touch insensitivity [22].

Overall, our data suggest that posterior touch stimuli induce phosphorylation of the membrane distal NPxY. The touch insensitivity in *pat-3(YYFF)* indicates that phosphorylation of both NPxY motifs may contribute to the mechanosensation. Mechanical stimuli might simultaneously or sequentially phosphorylate two NPxY motifs, transmitting mechanical information to mechanotransduction targets within the cell. The NPVY$^{804}$ motif appears to bind a downstream molecule, presumably, UNC-112/kindlin, which remains constitutively attached to phosphorylated NPVY$^{804}$. In contrast, phosphorylation of the proximal NPIY$^{792}$ inhibits binding to TLN-1/talin. We propose that

*pat-3(Y804E)* mechanosensation defect arises from impaired interaction with UNC-112/kindlin.

The touch insensitivity of *pat-3(Y792F) is* restricted to the posterior regions of the body. Phosphorylation of the proximal NPIY$^{792}$ may transiently occur in PLM or HSN neurons, affecting cytoskeleton dynamics via talin. However, disruptive or single non-phosphorylatable mutations in the distal motif, such as *pat-3(Y804A)* and *pat-3(Y804F)*, do not result in touch defects in either the anterior or posterior body. This suggests that these mutations have minimal impact on the involvement of distal NPxY in mechanosensation.

How does βPAT-3 integrin contribute to mechanosensation in neurons or muscles? One straightforward interpretation is that the NPxY mutants cause unknown muscle anomalies, thereby reducing the motor activity of muscles in response to touch stimuli. However, the βPAT-3 protein is expressed in all tissues, particularly muscles and neurons [9]. Therefore, one cannot rule out the potential role of βPAT-3 NPxY in neurons. Previous analysis shows that the *pat-3* integrin directs the posterior-to-anterior migration of PLM axons during the development [46], suggesting that the mechanosensation defect observed in NPxY mutants stems from impaired PLM axon outgrowth. Consequently, stranded PLM axons fail to detect touch stimuli in the posterior body. Another possibility is that integrin may act as a direct mediator of mechanotransduction, potentially interacting with MEC-4 or other touch receptors [47]. Tyrosine phosphorylation of the proximal NPIY$^{792}$ transiently occurs, facilitating interaction with MEC-4. Upon touch stimulation, the MEC-4 channel may induce phosphorylation of the proximal motif, subsequently triggering the release of neurotransmitters at the PLM synapse to inhibit motor neurons such as HSN [38,43].

In mammalian studies, β3 integrin YYFF knock-in mice exhibited a mild defect in clot retraction and a tendency to rebleed [8]. However, other studies with β1 YYFF knock-in mice failed to detect any developmental defects in the mutant animals [6]. In our study, we present egg-laying and mechanosensation phenotypes associated with the Y792F,

Y804E, and YYFF mutations. This suggests that the membrane-proximal and distal NPxY motifs in mice β1 or β3 integrin play a role in reproductive and sensory behaviors similar to those of βPAT-3 *C. elegans* integrin.

# EXPERIMENTAL PROCEDURES

*Animals and Genetics*

All animals were fed with *E. coli*, OP50, and cultured at room temperature (21°C to 23°C) at all times. *C. elegans* N2 worm, AH3437 GFP::*tln-1*, and *mec-4(u253),* were obtained from Caenorhabditis Genetics Center at St. Paul, MN. The CRISPR-Cas9 edited worms*, pat-3(kq8041, Y804A), pat-3(kq8042, Y804E),* and *pat-3(kq8043, Y804F)* were previously generated and described [12,48]. All *pat-3* NPxY mutants and other lines are listed in Supplementary Table 1 (Table S1).

Genetic double mutant lines (Table S1) were generated by crossing homozygote males from AH3437 GFP::*tln-1* [27] to each NPxY edited line hermaphrodite. From the F2 generation, a worm with 100% green (F3) progeny and the *pat-3* NPxY allele homozygosity (by PCR genotyping) was selected for further studies.

*Phenotype Analysis and Fluorescence Imaging.*

Fecundity analyses of N2, *pat-3 NPxY*, and other mutants were conducted as follows. Eggs were collected from worms grown on NGM plates (Day -2). After 48 hours (Day 0), the hatched larvae were transferred to individual NGM plates, with one worm per plate. At 72 hours (Day 1), each worm was transferred daily to a new NGM plate for four additional days. After the worm was removed and placed onto a new plate, the progeny on the previous plate were allowed to grow for one more day. The viable progeny were then stored at 4°C, and the number of progeny on each plate was subsequently counted and recorded for analysis.

For egg-laying assays, an adult worm was placed in 100 µl of M9 buffer per well in a 96-well microtiter plate containing fluoxetine (0.5 mg/ml, Sigma-Aldrich) or serotonin (3 mg/ml). After a 15-minute acclimation period, the number of eggs laid was counted 60 minutes later. For egg retention assays, eggs were transferred to an OP50-seeded plate and grown for four days at room temperature. Adult worms were then placed on a

microscope slide containing 50 to 100 µl of M9 buffer, and eggs were extruded using a 26-gauge needle. The extruded eggs were counted and categorized by developmental stage, with eggs at the bean-shaped or later embryonic stages scored as late-stage embryos.

For mechanosensation assays, following the protocol by Hobert *et al.* (1997), young adult animals that had been fed *E. coli* OP50 for two generations without starvation were gently stroked with eyebrow hairs ten times—five times on the anterior body and five times on the posterior body [23]. Responses such as backing movement to anterior touch and sprinting or twisting to posterior touch were scored as 1, while no responses to touch were scored as 0. Sample images were taken using a Nikon Eclipse Ni-U fluorescence microscope and a Coolsnap Dyno digital monochrome camera (Photomerics, Tucson, AZ). Photograph images were analyzed using NIS elements (Nikon, Melville, NY).

*The generation of CRISPR-Cas9 knock-in C. elegans*

The CRISPR-Cas9 system was used to edit the *pat-3* locus to create the *kq24*, YY792/804FF (YYFF) mutation, and other alleles. For *kq24*, the two crRNA, ZQPATY1(CGAGAACCCAATCTACAAAC) and ZQPAT3B (TTTAAAAATCCAGTATACGC) were obtained from the exon 8 of the *pat-3* gene covering the membrane-proximal and distal NPxY and purchased from IDT Inc., Coralville, IA. The homologous directed repair template (taaatttatcaaattatcattttcagAACGAGAATCCAATTTTTAAGCAAGCCACGACAACATTCA AGAACCCGGTTTTTGCAGGAAAAGCCAACTAAatagtttttatccttatatt) spans 48 bases upstream and 38 bases downstream of the target site, tyrosine ($Y^{792}$ and $Y^{804}$). Mutations modified the third position of codons in the crRNA target sequence to a synonymous codon. The repair DNA templates, crRNA, tracrRNA, and Cas9 nuclease were custom-made by IDT Inc., Coralville, IA. A mixture of template DNA, two crRNA (ZQAPTY1 and ZQPAT3B), tracrRNA (cat. no. 1073190), and Cas9 protein (cat. no. 1081058) was annealed at room temperature. The mixture was micro-injected into the

syncytial gonad of N2 animals (P0) with *dpy-10* co-CRISPR [49,50]. Homozygous mutants were crossed back to N2 two times. The mutation was confirmed by sequencing DNA molecules extracted from homozygous animals [12]. The generation of other edits was carried out similarly to the techniques mentioned above. The nucleotide sequences of crRNA and templates are listed in Supplementary Table S2 (Table S2).

*Statistical Analysis*

Statistical analysis of multiple *C. elegans* strains was conducted using All Pairwise Comparisons - Tukey HSD (Honestly Significant Difference) method [51]. The egg-laying assay utilized a Poisson regression model, while the regular and late-stage egg retention assays employed the Comparison of Means. A significance level was set at $p < 0.05$. Touch sensing assays were subjected to logistic regression and all pairwise comparisons for Tukey HSD. All data were analyzed using JMP Pro (version 17.0, SAS Institute, Cary, NC) software. Pairwise comparison data with $p > 0.05$ can be found in Supplementary Tables 3, 4, 5, and 6.

Acknowledgments

The Office of Engaged Learning at Baylor University URSA Research Fund supported this work. The *pat-3* mutants were generated for the BIO4108 Laboratory Class. The authors acknowledge Catherine Ravikumar, Arlyn Alcid, and Jeancarlo Gutierrez for their help during the initial stage of the project. The authors also appreciate Drs. Erin Cram and Ilya Ruvinsky for their comments on the initial draft.

## REFERENCES


1. Hynes RO. Integrins: bidirectional, allosteric signaling machines. *Cell*. Sep 20 2002;110(6):673-87.
2. Arnaout MA, Mahalingam B, Xiong JP. Integrin structure, allostery, and bidirectional signaling. *Annu Rev Cell Dev Biol*. 2005;21:381-410. https://doi.org10.1146/annurev.cellbio.21.090704.151217.
3. Qiu Z, Sheesley P, Ahn JH, Yu EJ, Lee M. A Novel Mutation in an NPXY Motif of beta Integrin Reveals Phenotypes Similar to him-4/hemicentin. *Front Cell Dev Biol*. 2019;7:247. https://doi.org10.3389/fcell.2019.00247.
4. Theodosiou M, Widmaier M, Bottcher RT, et al. Kindlin-2 cooperates with talin to activate integrins and induces cell spreading by directly binding paxillin. *Elife*. Jan 27 2016;5:e10130. https://doi.org10.7554/eLife.10130.
5. Sakai T, Jove R, Fassler R, Mosher DF. Role of the cytoplasmic tyrosines of b1A integrins in transformation by v-src. *Proceedings of the National Academy of Science, USA*. 2001;98(7):3808-3813.
6. Czuchra A, Meyer H, Legate KR, Brakebusch C, Fassler R. Genetic analysis of beta1 integrin "activation motifs" in mice. *J Cell Biol*. Sep 11 2006;174(6):889-99.
7. Meves A, Geiger T, Zanivan S, DiGiovanni J, Mann M, Fassler R. Beta1 integrin cytoplasmic tyrosines promote skin tumorigenesis independent of their phosphorylation. *Proc Natl Acad Sci U S A*. Sep 13 2011;108(37):15213-8. https://doi.org10.1073/pnas.1105689108.
8. Law DA, DeGuzman FR, Heiser P, Ministri-Madrid K, Killeen H, Phillips DR. Integrin cytoplasmic tyrosine motif is required for outside-in aIIbb3 signalling and platelet function. *Nature*. 1999;401:808-811.
9. Gettner SN, Kenyon C, Reichardt LF. Characterization of bpat-3 heterodimers, a family of essential integrin receptors in *C. elegan*s. *Journal of Cell Biology*. 1995;129:1127-1141.
10. Lee M, Cram EJ, Shen B, Schwarzbauer JE. Roles for beta(pat-3) integrins in development and function of Caenorhabditis elegans muscles and gonads. *J Biol Chem*. Sep 28 2001;276(39):36404-10. https://doi.org10.1074/jbc.M105795200 M105795200 [pii].
11. Itoh B, Hirose T, Takata N, et al. SRC-1, a non-receptor type of protein tyrosine kinase, controls the direction of cell and growth cone migration in C. elegans. *Development*. Dec 2005;132(23):5161-72. https://doi.org10.1242/dev.02103.
12. Hanna J, Ramani S, Williams T, et al. Three alleles in the pat-3 locus of Caenorhabditis elegans: mutations in the membrane-distal NPxY phosphotyrosine motif. *MicroPubl Biol*. Aug 15 2020;2020. https://doi.org10.17912/micropub.biology.000291.
13. Trent C, Tsung N, Horvitz HR. Egg-laying defective mutants of the nematode *C. elegans*. *Genetics*. 1983;104:619-647.
14. Moerman DG, Fire A. Muscle: Structure, function, and development. In: Riddle DL, ed. *C. elegans II*. Cold Spring Harbor, NY: Cold Spring Harbor Laboratory Press; 1997:417-470.

15. Lee M, Shen B, Schwarzbauer JE, Ahn J, Kwon J. Connections between integrins and Rac GTPase pathways control gonad formation and function in C. elegans. *Biochim Biophys Acta*. May 25 2005;1723(1-3):248-55. https://doi.orgS0304-4165(05)00009-7 [pii] 10.1016/j.bbagen.2005.01.003.
16. Qiu Z, Park A, Wang L, Wilsey R, Lee M. The RGD (Arg-Gly-Asp) is a potential cell-binding motif of UNC-52/PERLECAN. *Biochem Biophys Res Commun*. Jan 1 2022;586:143-149. https://doi.org10.1016/j.bbrc.2021.11.083.
17. Wilsey R, Hodge S, Kenney K, et al. Two alleles of unc-52 locus disrupting potential cell-binding motif of UNC-52. *MicroPubl Biol*. May 17 2020;2020. https://doi.org10.17912/micropub.biology.000250.
18. Minniti AN, Labarca M, Hurtado C, Brandan E. Caenorhabditis elegans syndecan (SDN-1) is required for normal egg laying and associates with the nervous system and the vulva. *J Cell Sci*. Oct 1 2004;117(Pt 21):5179-90. https://doi.org10.1242/jcs.01394.
19. Goodman MB. Mechanosensation. *WormBook*. 2006:1-14. https://doi.org10.1895/wormbook.1.62.1.
20. Chalfie M, Hart AC, Rankin CH, Goodman MB. Assaying mechanosensation. *WormBook*. Jul 31 2014. https://doi.org10.1895/wormbook.1.172.1.
21. Zuidema A, Wang W, Sonnenberg A. Crosstalk between Cell Adhesion Complexes in Regulation of Mechanotransduction. *Bioessays*. Nov 2020;42(11):e2000119. https://doi.org10.1002/bies.202000119.
22. Chen X, Chalfie M. Modulation of C. elegans touch sensitivity is integrated at multiple levels. *J Neurosci*. May 7 2014;34(19):6522-36. https://doi.org10.1523/JNEUROSCI.0022-14.2014.
23. Hobert O, Moerman DG, Clark KA, Beckerle MC, Ruvkun G. A conserved LIM protein that affects muscular adherens junction integrity and mechanosensory function in Caenorhabditis elegans. *J Cell Biol*. Jan 11 1999;144(1):45-57.
24. Williams BD, Waterston RH. Genes critical for muscle development and function in *Caenorhabditis elegans* identified through lethal mutations. *Journal of Cell Biology*. 1994;124:475-490.
25. Lin X, Qadota H, Moerman DG, Williams BD. *C. elegans* PAT-6/Actopaxin plays a critical role in the assembly of integrin adhesion complexes *in vivo*. *Current Biology*. 2003/5/27 2003;13(11):922-932.
26. Rogalski TM, Mullen GP, Gilbert MM, Williams BD, Moerman DB. The UNC-112 gene in *Caenorhabditis elegans* encodes a novel component of cell-matrix adhesion structure required for integrin localization in the muscle cell membrane. *Journal of Cell Biology*. 2000;150(1):253-264.
27. Walser M, Umbricht CA, Frohli E, Nanni P, Hajnal A. beta-Integrin de-phosphorylation by the Density-Enhanced Phosphatase DEP-1 attenuates EGFR signaling in C. elegans. *PLoS Genet*. Jan 2017;13(1):e1006592. https://doi.org10.1371/journal.pgen.1006592.
28. Trent C. *Genetic and behavioral studies of the egg-laying system in Caenorhabditis elegans* [Dissertation]. Cambridge, MA.: Massachusetts Institute of Technology.; 1983.
29. Choy RK, Thomas JH. Fluoxetine-resistant mutants in C. elegans define a novel family of transmembrane proteins. *Mol Cell*. Aug 1999;4(2):143-52. https://doi.org10.1016/s1097-2765(00)80362-7.

30. Ranganathan R, Sawin ER, Trent C, Horvitz HR. Mutations in the Caenorhabditis elegans serotonin reuptake transporter MOD-5 reveal serotonin-dependent and -independent activities of fluoxetine. *J Neurosci*. Aug 15 2001;21(16):5871-84. https://doi.org10.1523/JNEUROSCI.21-16-05871.2001.
31. Tanis JE, Moresco JJ, Lindquist RA, Koelle MR. Regulation of serotonin biosynthesis by the G proteins Galphao and Galphaq controls serotonin signaling in Caenorhabditis elegans. *Genetics*. Jan 2008;178(1):157-69. https://doi.org10.1534/genetics.107.079780.
32. Wood WB. The Nematode. *Caenorhabditis elegans*. *Cold Spring Harbor Laboratory Press*. 1988.
33. Schafer WF. Genetics of egg-laying in worms. *Annu Rev Genet*. 2006;40:487-509. https://doi.org10.1146/annurev.genet.40.110405.090527.
34. Chalfie M, Sulston JE, White JG, Southgate E, Thomson JN, Brenner S. The neural circuit for touch sensitivity in Caenorhabditis elegans. *J Neurosci*. Apr 1985;5(4):956-64.
35. Zhang M, Chung SH, Fang-Yen C, et al. A self-regulating feed-forward circuit controlling C. elegans egg-laying behavior. *Curr Biol*. Oct 14 2008;18(19):1445-55. https://doi.org10.1016/j.cub.2008.08.047.
36. Ravi B, Garcia J, Collins KM. Homeostatic Feedback Modulates the Development of Two-State Patterned Activity in a Model Serotonin Motor Circuit in Caenorhabditis elegans. *J Neurosci*. Jul 11 2018;38(28):6283-6298. https://doi.org10.1523/JNEUROSCI.3658-17.2018.
37. Goodman MB, Schwarz EM. Transducing touch in Caenorhabditis elegans. *Annu Rev Physiol*. 2003;65:429-52. https://doi.org10.1146/annurev.physiol.65.092101.142659 092101.142659 [pii].
38. Li W, Kang L, Piggott BJ, Feng Z, Xu XZ. The neural circuits and sensory channels mediating harsh touch sensation in Caenorhabditis elegans. *Nat Commun*. 2011;2:315. https://doi.org10.1038/ncomms1308.
39. Chalfie M. Touch receptor development and function in Caenorhabditis elegans. *J Neurobiol*. Oct 1993;24(10):1433-41. https://doi.org10.1002/neu.480241013.
40. Chalfie M, Au M. Genetic control of differentiation of the Caenorhabditis elegans touch receptor neurons. *Science*. Feb 24 1989;243(4894 Pt 1):1027-33.
41. O'Hagan R, Chalfie M, Goodman MB. The MEC-4 DEG/ENaC channel of Caenorhabditis elegans touch receptor neurons transduces mechanical signals. *Nat Neurosci*. Jan 2005;8(1):43-50. https://doi.orgnn1362 [pii] 10.1038/nn1362.
42. Carneiro AM, Cook EH, Murphy DL, Blakely RD. Interactions between integrin alphaIIbbeta3 and the serotonin transporter regulate serotonin transport and platelet aggregation in mice and humans. *J Clin Invest*. Apr 2008;118(4):1544-52. https://doi.org10.1172/JCI33374.
43. Ravi B, Nassar LM, Kopchock RJ, 3rd, Dhakal P, Scheetz M, Collins KM. Ratiometric Calcium Imaging of Individual Neurons in Behaving Caenorhabditis Elegans. *J Vis Exp*. Feb 7 2018;(132). https://doi.org10.3791/56911.
44. Dag U, Nwabudike I, Kang D, et al. Dissecting the functional organization of the C. elegans serotonergic system at whole-brain scale. *Cell*. Jun 8 2023;186(12):2574-2592 e20. https://doi.org10.1016/j.cell.2023.04.023.

45. Segalat L, Elkes DA, Kaplan JM. Modulation of serotonin-controlled behaviors by Go in Caenorhabditis elegans. *Science*. Mar 17 1995;267(5204):1648-51.
46. Gettner SN. *Isolation and functional analysis of Caenorhabditis elegans integrin bpat-3* [Dissertation]. San Francisco, CA: University of California; 1994.
47. Shakibaei M, Mobasheri A. Beta1-integrins co-localize with Na, K-ATPase, epithelial sodium channels (ENaC) and voltage activated calcium channels (VACC) in mechanoreceptor complexes of mouse limb-bud chondrocytes. *Histol Histopathol*. Apr 2003;18(2):343-51. https://doi.org10.14670/HH-18.343.
48. Park A, Qiu Z, Bumm J, Lee M. A novel mutation in unc-112/kindlin locus causes distal tip cell migration defects. *MicroPubl Biol*. Jun 8 2020;2020. https://doi.org10.17912/micropub.biology.000265.
49. Paix A, Folkmann A, Rasoloson D, Seydoux G. High Efficiency, Homology-Directed Genome Editing in Caenorhabditis elegans Using CRISPR-Cas9 Ribonucleoprotein Complexes. *Genetics*. Sep 2015;201(1):47-54. https://doi.org10.1534/genetics.115.179382.
50. Dickinson DJ, Goldstein B. CRISPR-Based Methods for Caenorhabditis elegans Genome Engineering. *Genetics*. Mar 2016;202(3):885-901. https://doi.org10.1534/genetics.115.182162.
51. Tukey JW. Comparing individual means in the analysis of variance. *Biometrics*. Jun 1949;5(2):99-114.
52. Francis R, Waterston RH. Muscle cell attachment in *Caenorhabditis elegans*. *Journal of Cell Biology*. 1991;114:465-479.

1 Figure 1.

2

| | |
|---|---|
| **H.S. β1A** | **$^{775}$WDTGENPIYKSAVTTVVNPKYEGK$^{798}$** |
| **βpat-3(+)** | **$^{784}$WDTNENPIYKQATTTFKNPVYAGKAN$^{809}$** |
| **βpat-3(Y792A)** | **$^{784}$WDTNENPIAKQATTTFKNPVYAGKAN$^{809}$** |
| **βpat-3(Y792F)** | **$^{784}$WDTNENPIFKQATTTFKNPVYAGKAN$^{809}$** |
| **βpat-3(YYFF)** | **$^{784}$WDTNENPIFKQATTTFKNPVFAGKAN$^{809}$** |
| **βpat-3(Y804A)** | **$^{784}$WDTNENPIYKQATTTFKNPVAAGKAN$^{809}$** |
| **βpat-3(Y804E)** | **$^{784}$WDTNENPIYKQATTTFKNPVEAGKAN$^{809}$** |
| **βpat-3(Y804F)** | **$^{784}$WDTNENPIYKQATTTFKNPVFAGKAN$^{809}$** |

3

4

5 Amino acid residues in βPAT-3 cytoplasmic tail sequence and their functions. The
6 amino acid sequence of the human β1A integrin CTD is aligned
7 with *PAT-3 (+),* wild-type CTD, and mutant CTD such as *pat-3(kq7921, Y792A), pat-*
8 *3(kq7923, Y792F), pat-3(kq24, YYFF), pat-3(kq8041, Y804A), pat-3(kq8042, Y804E),*
9 *and pat-3(kq8043, Y804F).* Reds indicate mutations.

10

Figure 2. *GFP::tln-1/talin* localization in *pat-3* NPxY mutants

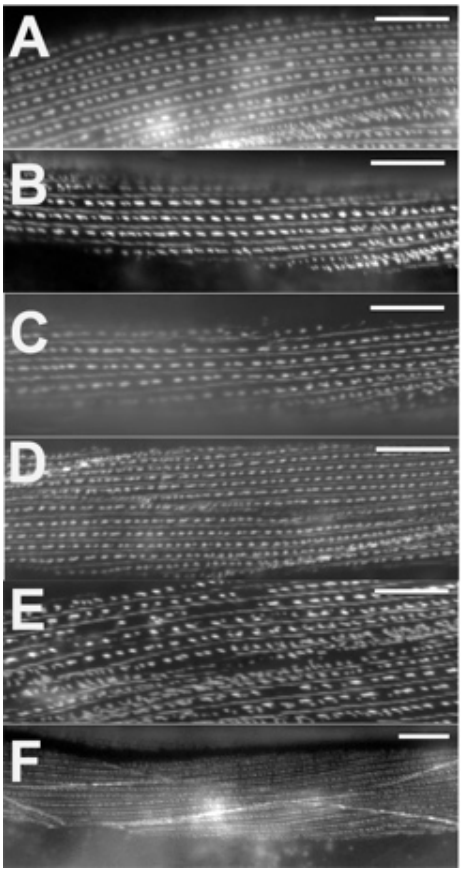


The six double mutants were generated by crossing GFP::*tln-1* to *pat-3* NPxY mutants. In every picture, horizontal dots represent dense bodies, and thin lines between the dense bodies represent M lines [52]. All images are taken under a 60X objective lens, except panel G (40X). Homozygous mutants are shown here. A. AH3437 *GFP::tln-1* body wall muscle of adult worm (control), B. *GFP::tln-1; pat-3(kq8042, Y804E),* C. *GFP::tln-1; pat-3(kq8041, Y804A),* D. *GFP::tln-1;pat-3(kq7923, Y792F),* E. *GFP::tln-1;pat-3(Y792A),* F. *GFP::tln-1;pat-3(YYFF)*. Bars = 10 µm.

1

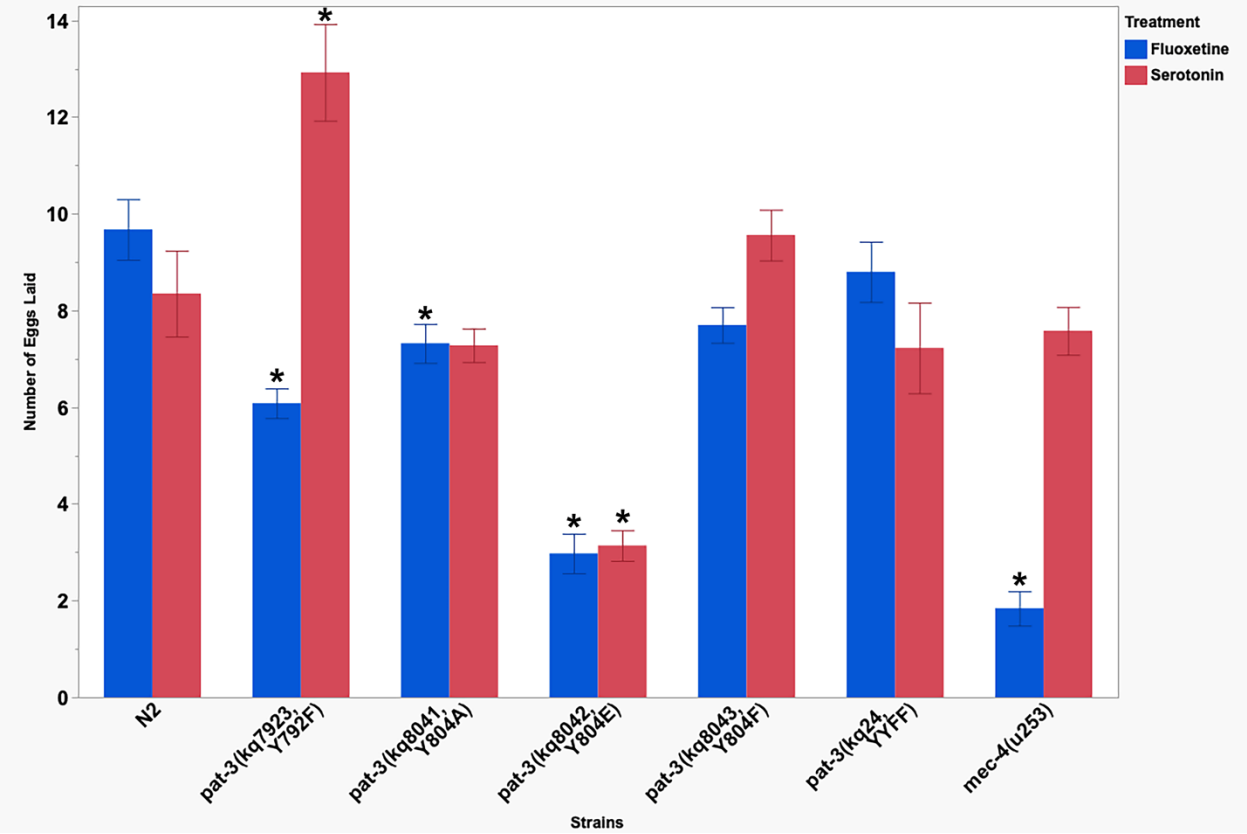


2

3 Figure 3. Egg laying assays of integrin mutants. Results significantly different from N2
4 were marked with * ($p < 0.05$). Brackets indicate significant differences between the
5 treatments. Multiple adult worms (n=40 or 50) were used for each experiment. *All
6 Pairwise Comparisons - Tukey HSD.

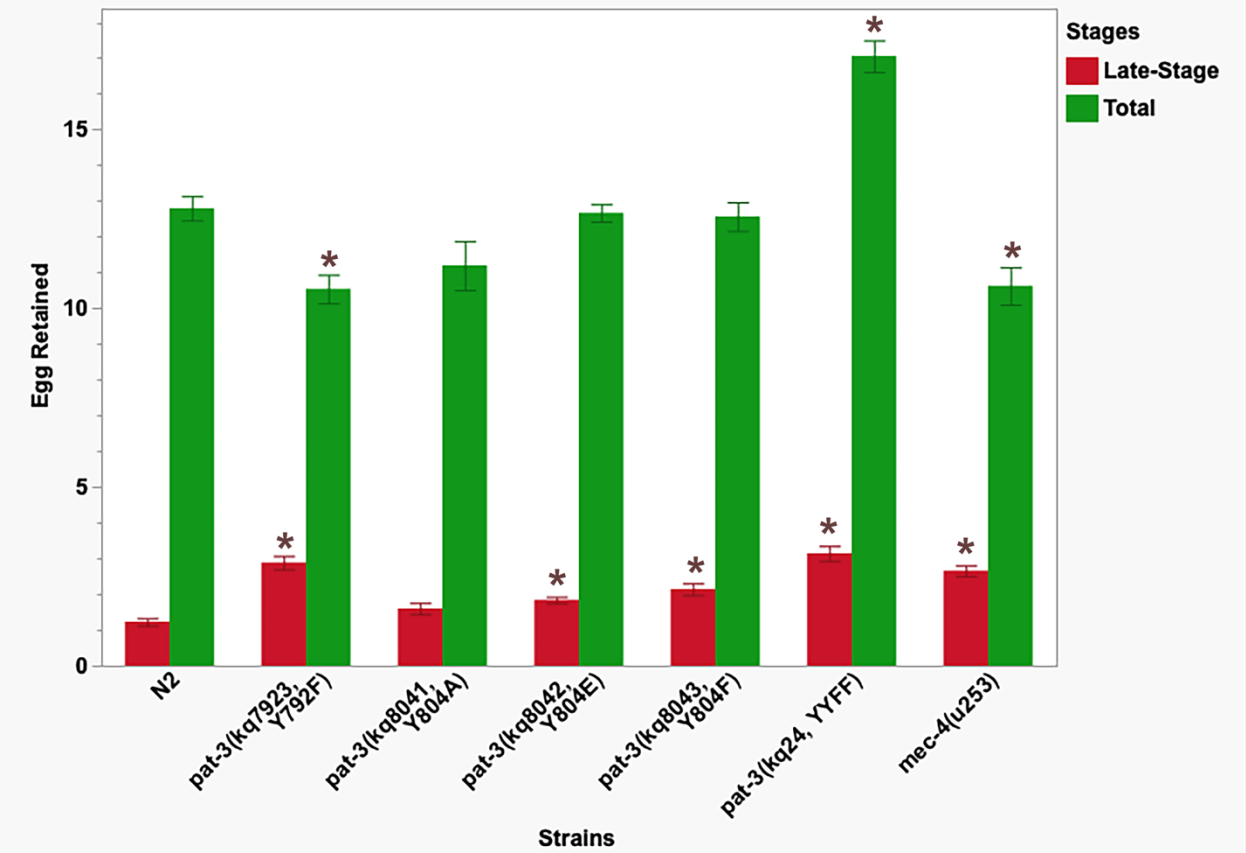


Figure 4. Egg retention assays of integrin mutants. Results significantly different from N2 were marked with * ($p < 0.05$). Multiple worms (n = 35 or 50) were used for each scoring. Green bars represent total eggs; red bars represent late-stage eggs. * All Pairwise Comparisons – Oneway analysis of variance.

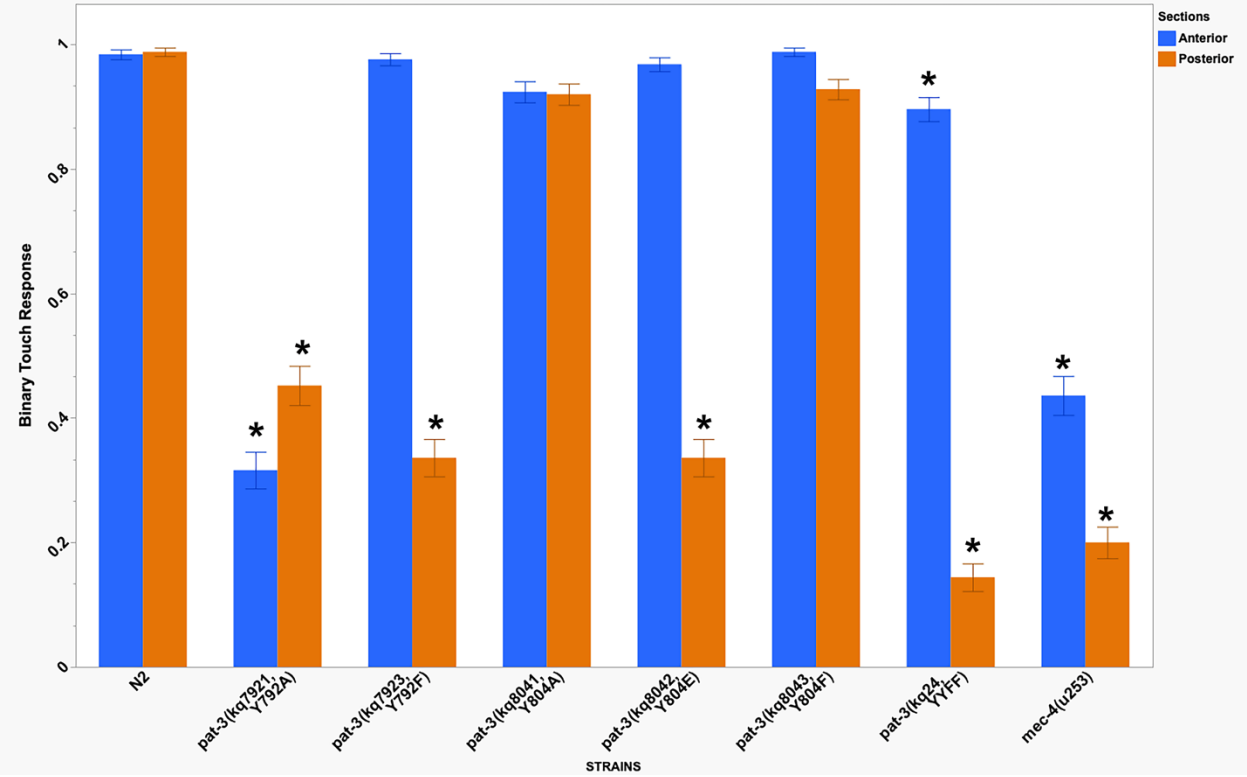


Figure 5. Mechanosensation analysis of *pat-3* NPxY mutants and *mec-4*. Results significantly different from N2 were marked with * ($p < 0.05$). All Pairwise Comparisons – Tukey HSD analyzed the averages of each test (n = 50).